

Magnetic structure of EuFe_2P_2 studied by neutron powder diffraction

D. H. Ryan,¹ J. M. Cadogan,² Shenggao Xu,³ Zhu'an Xu,³ and Guanghan Cao³

¹*Physics Department and Centre for the Physics of Materials, McGill University, Montreal H3A 2T8, Canada*

²*Department of Physics and Astronomy, University of Manitoba, Winnipeg, Manitoba R3T 2N2, Canada*

³*Department of Physics and State Key Lab of Silicon Materials, Zhejiang University, Hangzhou 310027, China*

(Received 8 December 2010; revised manuscript received 11 February 2011; published 13 April 2011)

A neutron powder diffraction study of EuFe_2P_2 at a wavelength of $2.3672(1) \text{ \AA}$ shows that the $6.6(3) \mu_B \text{ Eu}^{2+}$ moments order ferromagnetically at $T_C = 30(1) \text{ K}$ and are canted at an angle of $17(3)^\circ$ from the c axis. No evidence for the previously proposed antiferromagnetic or helimagnetic structures was found. The almost axial ferromagnetic structure of EuFe_2P_2 contrasts sharply with the planar antiferromagnetism seen in EuFe_2As_2 and many other europium–transition metal pnictides, suggesting a delicate interplay between the $\text{Eu } 4f$ and transition metal $3d$ electrons.

DOI: [10.1103/PhysRevB.83.132403](https://doi.org/10.1103/PhysRevB.83.132403)

PACS number(s): 75.25.-j, 75.50.Bb

I. INTRODUCTION

The pnictide intermetallic compounds RT_2Pn_2 (R = rare earth; T = transition metal Fe , Co , Ni , Pd ; Pn = pnictide P , As) crystallize in the tetragonal ThCr_2Si_2 -type structure (space group $I4/mmm$: No. 139)¹ and exhibit a rich variety of magnetic and transport phenomena. Following the initial characterization of these materials over twenty years ago,^{2,3} interest in the pnictide members of this much larger 1-2-2 compound family has been revived by the recent discovery of a large group of iron-pnictide-based superconductors. The RFe_2Pn_2 series provide a remarkable system in which to investigate the impact and role of P/As substitution as the same range of behavior seen in the $\text{CeFe}(\text{As},\text{P})\text{O}$ system, namely from a nearly ferromagnetic (FM) heavy fermion metal in CeFePO ⁴ to superconductivity in $\text{CeFeAsO}_{1-x}\text{F}_x$,⁵ is also seen in the EuFe_2Pn_2 systems.^{6,7}

A frequent limitation in many studies of the magnetic properties of europium-based compounds is the absence of direct measurements of the actual magnetic structure adopted by the Eu sublattice in the compounds. This absence arises from the perception that powder diffraction with thermal neutrons, the most direct and widely used technique for establishing magnetic structures, is impractical because of the large thermal neutron absorption cross section for natural europium ($\sigma_{\text{abs}} = 4530 \pm 40 \text{ b}$, due to the high absorption cross section of ^{151}Eu , the isotope that makes up almost half of natural europium). Two common solutions are to use “hot” neutrons ($\lambda < 1 \text{ \AA}$) to reduce the absorption effects but at the cost of greatly diminished resolution, or resonant x-ray scattering to avoid the absorption problem altogether. Both have been employed to study the europium pnictides. Single crystal neutron diffraction at a neutron wavelength of 0.85 \AA showed that the Eu moments adopt an incommensurate planar spiral structure in EuCo_2P_2 ,⁸ while both hot neutrons⁹ and resonant x-ray scattering¹⁰ showed EuFe_2As_2 to be a planar antiferromagnet (AFM). A recent resonant x-ray scattering of EuRh_2As_2 showed evidence for both commensurate and incommensurate planar ordering.¹¹ Remarkably, an extensive study of the magnetic and transport properties of EuFe_2P_2 ⁶ has shown that the iron does not order and that not only is this system probably ferromagnetic, but that the Eu moments are ordered close to the c axis, i.e., essentially perpendicular to

the ordering plane seen in all of the related europium pnictides studied so far.

We report here a neutron powder diffraction study at a thermal wavelength of $2.3672(1) \text{ \AA}$ using a recently developed large-area flat-plate geometry¹² that greatly reduces the absorption problems associated with europium compounds. The approach can even be used to study compounds that are rich in gadolinium ($\sigma_{\text{abs}} = 49700 \pm 125 \text{ b}$).^{13,14} We show that EuFe_2P_2 is indeed ferromagnetic with Eu^{2+} moments of $6.6(3) \mu_B$ oriented close to the c axis. We confirm the canted structure implied by local (^{57}Fe and ^{151}Eu Mössbauer spectroscopy) measurements in which a canting angle of $20(5)^\circ$ was found by considering the orientation of the hyperfine magnetic fields within the principal axis frame of the electric field gradient.⁶ However, we find no evidence for a more complex helimagnetic structure.⁶

II. EXPERIMENTAL METHODS

The polycrystalline sample of EuFe_2P_2 was synthesized by solid state reaction between EuP and Fe_2P . The details of the preparation and pre-synthesis of the phosphides have been reported previously.^{6,15} The sample was almost single phase, with about 2 wt % of an Fe_3P impurity observed in the neutron diffraction patterns.

For the neutron diffraction measurements, 1.7 g (slightly less than a $1/e$ thickness for absorption) was spread across a $2 \text{ cm} \times 8 \text{ cm}$ area on a $600 \mu\text{m}$ thick single-crystal silicon wafer and immobilized using a 1% solution of GE-7031 varnish in toluene/methanol (1:1).¹² Neutron diffraction experiments were carried out on the C2 multiwire powder diffractometer (DUALSPEC) at the NRU reactor, Canadian Neutron Beam Centre, Chalk River, Ontario. A relatively long neutron wavelength of $2.3672(1) \text{ \AA}$ was used so that low-angle peaks due to any AFM ordering would be well clear of any direct beam contamination. The plate was oriented with its surface normal parallel to the incident neutron beam in order to maximize the total flux onto the sample and the measurements were made in transmission mode. Temperatures down to 3.6 K were obtained using a closed-cycle refrigerator with the sample in a partial pressure of helium to ensure thermal uniformity. All full-pattern magnetic and structural refinements employed the FullProf/WinPlotr suite^{16,17} with neutron scattering length

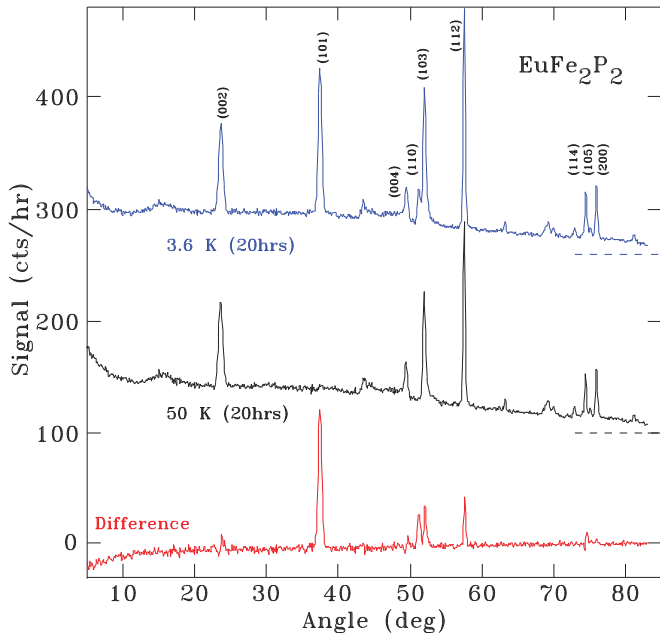


FIG. 1. (Color online) Powder neutron diffraction patterns for EuFe_2P_2 taken at a wavelength of $2.3672(1)$ Å above (50 K) and below (3.6 K) T_C showing the development of magnetic scattering on cooling. The intensity changes can be seen more clearly in the difference pattern shown at the bottom of the figure. The indexing of the strongest peaks is given on the 3.6 K pattern. The two measured patterns have been offset vertically for visualization purposes; however, the dashed lines at the right show the locations of the actual zero values in each case. The features near $2\theta = 45^\circ$ and $2\theta = 70^\circ$ are instrumental artifacts.

coefficients for natural Eu taken from the tabulation by Lynn and Seeger.¹⁸

III. RESULTS

The diffraction pattern taken at 50 K (i.e., above T_C) is presented in Fig. 1 and clearly shows the nuclear Bragg peaks of the EuFe_2P_2 phase, demonstrating that neutron powder diffraction does indeed yield a significant signal from europium-based compounds. The crystallographic data for EuFe_2P_2 , derived from the refinement of the 50 K neutron diffraction pattern, are given in Table I. The lattice parameters at 50 K are $a = 3.8165(7)$ Å and $c = 11.166(3)$ Å. The conventional R factors are $R(\text{Bragg}) = 7.6\%$ and $R(F) = 7.0\%$.

Cooling below T_C leads to many changes in the observed diffraction pattern, and while several peaks clearly grow in intensity, there are no new peaks (i.e., none that would be forbidden by the crystallographic $I4/mmm$ structure). In particular, there are no new peaks below the (0 0 2) peak near $2\theta = 24^\circ$, which would signal the development of commensurate or incommensurate AFM ordering, nor

TABLE I. Crystallographic data for EuFe_2P_2 obtained by refinement of the 50 K neutron powder diffraction pattern.

Atom	Site	x	y	z
Eu	2a	0	0	0
Fe	4d	0	$\frac{1}{2}$	$\frac{1}{4}$
P	4e	0	0	0.360(2)

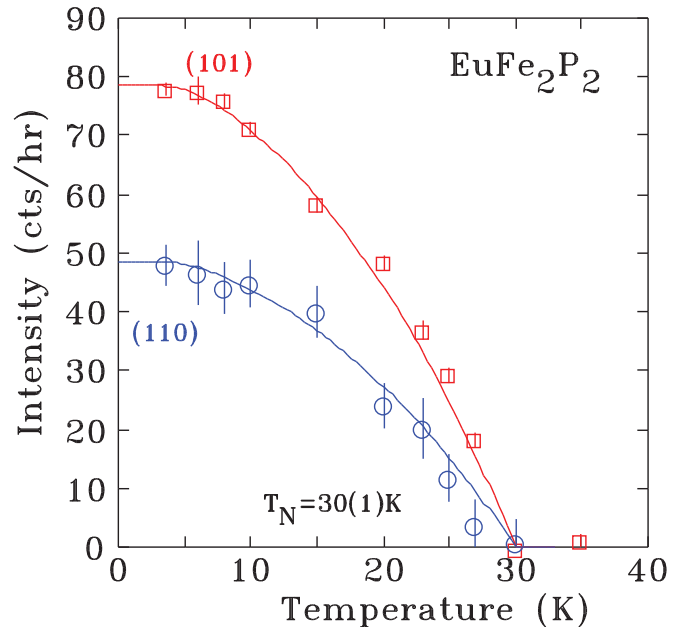


FIG. 2. (Color online) Intensities of the (1 0 1) and (1 1 0) peaks for EuFe_2P_2 as functions of temperature showing an average Curie temperature of $30(1)$ K. The solid lines are fits to squared $J = \frac{7}{2}$ Brillouin functions (the intensity is proportional to the moment squared). The intensity of the (1 1 0) peak has been scaled up by a factor of 4 for clarity.

do we observe any satellite peaks around the main peaks which would indicate helimagnetic ordering, as previously proposed.⁶ The changes are emphasized in the difference pattern shown at the bottom of Fig. 1 where the dramatic growth of the (1 0 1) peak is the most striking feature. The much smaller increase in the intensity of the (0 0 2) peak is less obvious but is far more important as it indicates that the Eu^{2+} moments *cannot* be strictly parallel to the c axis: The FM order must be canted away from the c axis by some small angle as previously deduced from ^{57}Fe and ^{151}Eu Mössbauer spectroscopy.⁶ Finally, the downturn in the difference pattern below $2\theta = 30^\circ$ in Fig. 1 is due to the loss of incoherent paramagnetic scattering from the Eu^{2+} ions as the FM order develops below T_C . This serves to underline the strength of the magnetic scattering from this system.

In Fig. 2 we follow the temperature dependence of the intensities of two of the clearest peaks which allows us to determine the magnetic ordering temperature as $30(1)$ K. While there are no apparent breaks in the behavior that would suggest the presence of a second transition below T_C , we note that the strongest magnetic reflection [the (101) in Fig. 1] contains both axial and planar components and so is not very sensitive to the canting of the Eu^{2+} moments. Furthermore, the magnetic contribution to the (002) reflection, which allows us to determine the canting angle, is relatively small, so we cannot rule out the possibility that the initial FM ordering at T_C is axial and that a further canting transition occurs below it.

Since a helimagnetic structure has been suggested for EuFe_2P_2 ,⁶ we simulated a variety of magnetic structures that combine FM and AFM ordering in order to determine their impact on the diffraction pattern and formally rule them out before proceeding to the final analysis. In what

follows we consider only AFM ordering perpendicular to the c axis, as EuFe_2P_2 has been shown to be dominated by FM order⁶ and examination of our diffraction data places this FM ordering parallel to the c axis. The simplest AFM structure is formed by canting the body-center and cell-corner Eu moments away from the c axis, but in opposite directions. This makes the two Eu moments inequivalent, violating the I -centering translational symmetry of the crystallographic cell and releasing the $h + k + l = 2n$ constraint on the magnetic scattering. Simulations with $7 \mu_B$ Eu moments canted by $\pm 20^\circ$ from the c axis (to be consistent with the earlier Mössbauer work⁶) lead to substantial new peaks, with the $(0\ 0\ 1)$ at $2\theta \sim 12^\circ$ predicted to be comparable in strength to the $(0\ 0\ 2)$ nuclear peak at $2\theta \sim 24^\circ$. No such peak is observed and our data allow us to place the maximum possible canting angle for this test structure at 2° . The next simplest structure involves doubling the unit cell along the c axis by reversing the canting direction as one moves along the c axis from cell to cell. This leads to the development of a $(0\ 0\ \frac{1}{2})$ peak that dominates the pattern at $2\theta \sim 6^\circ$, being about *twice* the intensity of the $(0\ 0\ 2)$ nuclear peak. This peak is clearly absent (see Fig. 1) and the maximum possible canting angle for this test structure is $\sim 1^\circ$. The two foregoing commensurate structures can be characterized by a propagation vector of $(0\ 0\ k_z)$, where k_z is 1 and 0.5 respectively. This description can be generalized to include incommensurate, helimagnetic structures that exhibit diffraction patterns with a strong fundamental peak at $(0\ 0\ k_z)$ and weaker satellite peaks at $(h\ k\ l \pm k_z)$ that decorate the existing magnetic peaks. While the fundamental is quickly lost into the straight-through beam as k_z decreases through about 0.3, the intensity in that peak is still drawn from others in the pattern, and assuming a helimagnetic structure with an unobservable fundamental (i.e., $k_z < 0.3$) leads to unrealistic europium moments of $\sim 12 \mu_B$. Constraining the europium moment to $7 \mu_B$ leads to a maximum canting angle in a helimagnetic structure of $< 3^\circ$, with $k_z < 0.3$. Thus, in each case considered here, not only do we see no evidence to support the proposed structure, but the maximum possible canting angle is inconsistent with both ^{151}Eu and ^{57}Fe Mössbauer data.⁶ We therefore eliminate them from further consideration and proceed to an analysis in terms of FM ordering.

The refinement of the diffraction pattern obtained at 3.6 K is shown in Fig. 3. Earlier ^{57}Fe Mössbauer work showed no evidence for magnetic ordering of the iron⁶ so the magnetic contribution from the iron sites was assumed to be zero in our analysis. No misfit resulting from this choice was detected. The R factors were $R(\text{Bragg}) = 6.5\%$, $R(F) = 4.0\%$, and $R(\text{mag}) = 6.3\%$. Both a full pattern refinement and simulations of the magnetic contributions to the $(0\ 0\ 2)$ and $(1\ 0\ 1)$ reflections yield a canting angle of $17(3)^\circ$. This is fully consistent with the $20(5)^\circ$ derived from ^{151}Eu Mössbauer and $15(5)^\circ$ derived from ^{57}Fe Mössbauer.⁶ Our refinement of the 3.6 K pattern yields an Eu^{2+} magnetic moment of $6.6(3) \mu_B$ which is canted away from the tetragonal c axis by $17(3)^\circ$. This magnetic moment is close to the $7 \mu_B$ expected for the $J = \frac{7}{2} \text{Eu}^{2+}$ ion, confirming the divalence of the Eu ions.

The magnetic structure of EuFe_2P_2 contrasts sharply with that of EuFe_2As_2 which serves as a parent material for a family of high-temperature superconductors. First, the Fe sublattice in the phosphide is nonmagnetic in the whole temperature

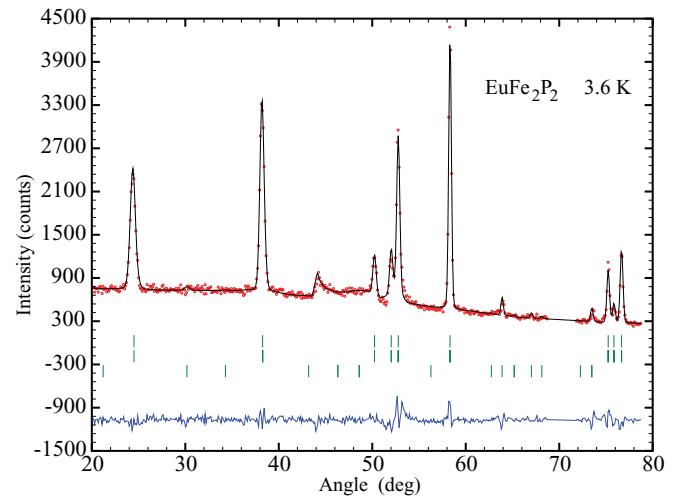


FIG. 3. (Color online) Refined diffraction pattern for EuFe_2P_2 obtained at 3.6 K. The solid line is a full-profile refinement of the nuclear and magnetic contributions. Three rows of Bragg markers are shown: (top) nuclear contribution, (middle) magnetic contribution, (bottom) Fe_3P impurity of 2 wt %. The residuals are plotted at the bottom of the figure. Note that since the magnetic order is ferromagnetic, there are no new Bragg peaks associated with it. The instrumental artifacts near $2\theta = 45^\circ$ and 70° were not included in the refinement.

above 2 K, contrasting with the collinear antiferromagnetic (AFM) ordering below 190 K in the arsenide.^{9,10} Second, the Eu sublattice orders ferromagnetically below 30 K with the moments nearly perpendicular to the basal planes in the phosphide, in contrast to the A-type AFM ordering^{7,19} below 19 K with the moments parallel to the crystallographic a axis^{9,10} seen in the arsenide. It is interesting that nickel doping of EuFe_2As_2 both suppresses the iron ordering and converts the Eu sublattice ordering from antiferromagnetic to ferromagnetic²⁰ (there is, unfortunately, no determination of the ferromagnetic ordering direction as yet) strongly suggesting that a common mechanism may be at work.

While the AFM-to-FM crossover can be qualitatively explained in terms of changes in the Ruderman-Kittel-Kasuya-Yosida (RKKY) interaction,^{6,21} resulting from a slight change in interatomic distances or electron density associated with the substitution of phosphorus for arsenic, the origin of the change in the europium ordering direction remains unclear. We note that the line joining a corner Eu atom to the body-centered Eu atom makes an angle of 26° with the c axis, roughly coincident with the spin-canting angle revealed by the previous Mössbauer study⁶ and the present work. While the RKKY interaction is fundamentally isotropic, it is possible that the covalency increase in going from As to P may introduce some weak directionality to the exchange. There may also be a contribution from the ordered iron moments in EuFe_2As_2 as both the iron and Eu moments order along the a axis, and if the iron ordering is weakened by nickel doping, the europium ordering becomes ferromagnetic,²⁰ suggesting that the electronic and magnetic states of the Fe-Pn layers may govern the magnetic structure of the Eu sublattice. Unfortunately no information about the actual ordering direction in $\text{EuFe}_{2-x}\text{Ni}_x\text{As}_2$ is currently available.

IV. CONCLUSIONS

We have demonstrated that neutron powder diffraction can indeed be performed on Eu-based compounds at thermal wavelengths and that it readily yields data of sufficient quality to enable a magnetic structure determination. We have studied the magnetic order of the pnictide intermetallic EuFe_2P_2 . At 3.6 K, well below the Curie temperature of 30(1) K, the 6.6(3) μ_B Eu^{2+} magnetic moments are canted away from the tetragonal c axis by 17(3) $^\circ$. We find no evidence for antiferromagnetic or helimagnetic contributions to the magnetic order.

ACKNOWLEDGMENTS

J.M.C. acknowledges support from the Canada Research Chairs program. Financial support for various stages of this work was provided by the Natural Sciences and Engineering Research Council of Canada and Fonds Québécois de la Recherche sur la Nature et les Technologies. G.C. acknowledges the support from the National Basic Research Program of China (Grant No. 2010CB923003) and the National Science Foundation of China (Grant No. 10934005).

-
- ¹R. Marchand and W. Jeitschko, *J. Solid State Chem.* **24**, 351 (1978).
²E. Mörsen, B. D. Mosel, W. Müller-Warmuth, M. Reehuis, and W. Jeitschko, *J. Phys. Chem. Solids* **49**, 785 (1988).
³H. Raffius, E. Mörsen, B. D. Mosel, W. Müller-Warmuth, W. Jeitschko, L. Terbüchte, and T. Vomhof, *J. Phys. Chem. Solids* **54**, 135 (1993).
⁴E. M. Brüning, C. Krellner, M. Baenitz, A. Jesche, F. Steglich, and C. Geibel, *Phys. Rev. Lett.* **101**, 117206 (2008).
⁵G. F. Chen, Z. Li, D. Wu, G. Li, W. Z. Hu, J. Dong, P. Zheng, J. L. Luo, and N. L. Wang, *Phys. Rev. Lett.* **100**, 247002 (2008).
⁶C. Feng, Z. Ren, S. Xu, S. Jiang, Z. Xu, G. Cao, I. Nowik, I. Felner, K. Matsubayashi, and Y. Uwatoko, *Phys. Rev. B* **82**, 094426 (2010).
⁷Z. Ren, Z. Zhu, S. Jiang, X. Xu, Q. Tao, C. Wang, C. Feng, G. Cao, and Z. Xu, *Phys. Rev. B* **78**, 052501 (2008).
⁸M. Reehuis, W. Jeitschko, M. Möller, and P. Brown, *J. Phys. Chem. Solids* **53**, 687 (1992).
⁹Y. Xiao, Y. Su, M. Meven, R. Mittal, C. M. N. Kumar, T. Chatterji, S. Price, J. Persson, N. Kumar, S. K. Dhar *et al.*, *Phys. Rev. B* **80**, 174424 (2009).
¹⁰J. Herrero-Martín, V. Scagnoli, C. Mazzoli, Y. Su, R. Mittal, Y. Xiao, T. Brueckel, N. Kumar, S. K. Dhar, A. Thamizhavel *et al.*, *Phys. Rev. B* **80**, 134411 (2009).
¹¹S. Nandi, A. Kreyssig, Y. Lee, Y. Singh, J. W. Kim, D. C. Johnston, B. N. Harmon, and A. I. Goldman, *Phys. Rev. B* **79**, 100407 (2009).
¹²D. H. Ryan and L. M. D. Cranswick, *J. Appl. Crystallogr.* **41**, 198 (2008).
¹³J. M. Cadogan, D. H. Ryan, M. Napoletano, P. Riani, and L. M. D. Cranswick, *J. Phys. Condens. Matter* **21**, 124201 (2009).
¹⁴D. H. Ryan, J. M. Cadogan, L. M. D. Cranswick, K. A. Gschneidner, V. K. Pecharsky, and Y. Mudryk, *Phys. Rev. B* **82**, 224405 (2010).
¹⁵Z. Ren, Q. Tao, S. Jiang, C. Feng, C. Wang, J. Dai, G. Cao, and Z. Xu, *Phys. Rev. Lett.* **102**, 137002 (2009).
¹⁶J. Rodríguez-Carvajal, *Physica B* **192**, 55 (1993).
¹⁷T. Roisnel and J. Rodríguez-Carvajal, *Mater. Sci. Forum* **378-81**, 118 (2001).
¹⁸J. E. Lynn and P. A. Seeger, *At. Data Nucl. Data Tables* **44**, 191 (1990).
¹⁹S. Jiang, Y. Luo, Z. Ren, Z. Zhu, C. Wang, X. Xu, Q. Tao, G. Cao, and Z. Xu, *New J. Phys.* **11**, 025007 (2009).
²⁰Z. Ren, X. Lin, Q. Tao, S. Jiang, Z. Zhu, C. Wang, G. Cao, and Z. Xu, *Phys. Rev. B* **79**, 094426 (2009).
²¹I. Nowik, I. Felner, Z. Ren, Z. A. Xu, and G. H. Cao, *J. Phys. Conf. Ser.* **217**, 012121 (2010).